Remote Sensing of Environment 114 (2010) 211–220

Contents lists available at ScienceDirect

Remote Sensing of Environment

journal homepage: www.elsevier.com/locate/rse

Ecosystem functioning of protected and altered Mediterranean environments: A remote sensing classification in Doñana, Spain

Néstor Fernández [a,*], José M. Paruelo [b,c], Miguel Delibes [a]

[a] Department of Conservation Biology, Doñana Biological Station, Spanish Council for Scientific Research CSIC, Av. Américo Vespucio s/n, 41092 Sevilla, Spain
[b] Laboratorio de Análisis Regional y Teledetección, Facultad de Agronomía e IFEVA, Universidad de Buenos Aires and CONICET, Av. San Martín 4453, 1417 Buenos Aires, Argentina
[c] Departamento de Métodos Cuantitativos y Sistemas de Información, Facultad de Agronomía e IFEVA, Universidad de Buenos Aires and CONICET, Av. San Martín 4453, 1417 Buenos Aires, Argentina

ARTICLE INFO

Article history:
Received 2 June 2009
Received in revised form 24 August 2009
Accepted 6 September 2009

Keywords:
Albedo
Doñana
Ecological classification
Evapotranspiration
fPAR
Land use change
Landsat
NDVI
Primary production
Protected areas

ABSTRACT

Spatial heterogeneity in ecosystem functioning is a key component of ecological variability requiring special attention in the context of global change. A large history of human use has produced high physiognomic heterogeneity in Mediterranean ecosystems. However, the consequences for ecosystem functioning remain insufficiently understood. We analyzed spectral indicators of matter and energy fluxes in the land surface to classify the functional ecosystem heterogeneity in a Mediterranean region covering different management histories and protection types. We specifically analyzed the spatial variability in seasonal and annual patterns in the Normalized Difference Vegetation Index (NDVI), surface temperature (T_s) and albedo from five Landsat ETM images. Then we classified numerically this variability into ecosystem functional types (EFTs) and explored their seasonal dynamics in terms of photosynthetic radiation absorption and evapotranspiration. We identified eight main EFTs with ecologically relevant differences including contrasting dynamics in fPAR seasonality, great variation in incoming radiation reflection and differing evapotranspiration rates, particularly during the water-limitation period. Functional variability in natural vegetation mostly consisted in dissimilar annual rates of NDVI and albedo, whereas differences in seasonality were more evident in transformed areas. Similarly, the spatial distribution of EFTs was partly associated to protection, with two EFTs exclusive of protected areas and comparatively higher functional diversity in humanized areas. Landform effects on water availability in protected areas and human activities under different ecological settings were seemingly responsible for the large functional diversity of the region. We advocate for the explicit incorporation of multifunctional ecosystem heterogeneity in ecosystem management and monitoring designs.

1. Introduction

Different drivers of current environmental change are rapidly degrading terrestrial ecosystems at regional and global levels (Millennium Ecosystem Assessment, 2005). In this context, the importance of characterizing ecosystem heterogeneity attending the composition, structure and functioning is well recognized in both management and conservation (Noss, 1990; Christensen et al., 1996). Recent advances in remote sensing have greatly contributed to map the physiognomic heterogeneity of ecosystems and their alteration both in space and time (e.g. Kerr & Ostrovsky, 2003). This has improved our capacity to understand the magnitude of human impacts on terrestrial ecosystems like the fragmentation and degradation of forests and wetlands, increases in the proportion of land dedicated to crops, expansion of deserts and the erosion of species habitats. However, patterns in ecosystem functioning and their changes still receive comparatively less attention among managers and conservationists, perhaps because they are less intuitive and more difficult to quantify. In recent years, ecosystem scientists are emphasizing the importance of incorporating the analysis and monitoring of carbon gains, nutrient cycling and water dynamics in regional and local-scale conservation programs, e.g. in protected areas (Paruelo et al., 2005; Crabtree et al., 2009). Expanding these approaches is challenging but critical for understanding and preserving the integrity of biological communities, ecosystem services and climate (Vitousek, 1994; Hooper et al., 2005).

Regional variability in ecosystem functioning depends on a complex combination of factors including the level of resources and regulators, the biogeographical context, the local history of environmental change and their interactions (Melillo et al., 1993; DeFries et al., 1999). This complexity limits the usefulness of general predictions to address local or regional ecosystem functional responses to the different drivers of environmental change. For example, analyses of land use change in different regions – mostly

* Corresponding author.
E-mail address: nestor@ebd.csic.es (N. Fernández).

0034-4257/$ – see front matter © 2009 Elsevier Inc. All rights reserved.
doi:10.1016/j.rse.2009.09.001

conversion of native vegetation to cropland – have shown both increases and decreases in primary production depending on ecological settings, the structure of the original vegetation and the intensity of land transformation (Paruelo et al., 2004a; Bradford et al., 2005). Uncertainties about the direction of land use effects on carbon gains illustrate the difficulty of formulating region-specific predictions about ecosystem functional responses to different regulators. There is a need for advancing in the quantification of regional-scale variability in ecosystem functioning, integrating matter and energy patterns, variability in vegetation physiognomy and other aspects of ecosystem structure, and their associations with human activities (Paruelo et al., 2004b). Although various remote sensing studies have found some degree of correspondence between ecosystem structure and functioning (e.g. Gould, 2000; Paruelo et al., 2001a), there is a general deficiency of knowledge about the nature and intensity of these relationships in most environments including Mediterranean ecosystems.

We propose that classification schemes able to incorporate multiple functioning properties can greatly contribute to characterize ecosystem heterogeneity and responses to environmental change, both in time and space. A regional-scale functional characterization of ecosystems requires the identification of matter and energy flux dynamics that in general are not easy to perceive. Remote sensing techniques allow quantifying key components of these fluxes and overcome some of the previous limitations imposed by the scale mismatch between field-based estimates and the spatial extent required in regional analyses. Thus, the analysis of vegetation indices (e.g. the normalized difference vegetation index NDVI) has provided critical information on ecosystem dynamics and their environmental and human controls, for example revealing the key impact of human transformations on the seasonal dynamics of aboveground net primary production (Guerschman et al., 2003; Bradford et al., 2006). Broad spatial coverage and ecological significance make these spectral indices suitable for developing process-based, broad-scale classifications of ecosystems grounded on their functioning properties. Based on this idea, Soriano and Paruelo (1992) and Paruelo et al. (2001b) introduced the concept of ecosystem functional type (EFT) to identify similarly functioning ecosystems according to patterns in NDVI. Ecologists and conservationists have widely recognized the practical utility of exploring patterns in vegetation indices since then (e.g. Turner et al., 2003; Cohen & Goward, 2004; Pettorelli et al., 2005) but further advances are required for a comprehensive characterization of ecosystems attending, additionally, to their contribution to water and energy balances in the land surface (e.g. Chapin et al., 2008).

Here we focused on multifunctional properties of ecosystems to develop a functional classification of a Mediterranean region comprising different protection levels. Mediterranean ecosystems have been extensively analyzed before using remote sensing mostly to achieve physiognomic classifications of vegetation at various spatial scales, for productivity and biomass monitoring, and for evaluating changes in vegetation cover associated to degradation processes (e.g. Shoshany, 2000; Hostert et al., 2003; Camacho-De Coca et al., 2004; Hill et al., 2008). We specifically aimed to address the following questions: (1) Is local-scale variability in ecosystem functioning ecologically relevant (e.g. as compared with broader-scale patterns in the Mediterranean and other regions)? Can this variability be synthesized into ecologically differentiated functional groups? (2) Do traditional structural descriptions of ecosystems reflect their functional heterogeneity? (3) How does land protection and human use intensity affect functional ecosystem heterogeneity? We identified ecosystem functional types based on seasonal and yearly functional parameters derived from NDVI, surface temperature (T_s) and albedo. Altogether, these indices capture critical aspects of carbon, energy and water fluxes in ecosystems, being NDVI a surrogate of carbon gains, T_s an indicator of energy partition into sensible and latent heat flux and albedo a key component of the radiation balance. Additionally we analyzed, for the different ecosystem functional types, seasonal patterns in evapotranspiration (ETP) and the fraction of photosynthetically active radiation absorbed by vegetation (fPAR). Lastly, we studied the correspondence between functional and structural descriptions of ecosystem heterogeneity and the effects of land use on ecosystem functioning.

2. Methods

2.1. Study region

We conducted this study in the Doñana region in southwestern Spain (38°13′ N, 48°10′ W), an area of 3560 km^2 that includes a wide representation of protection levels (from strict protection to unprotected) together with a rich variety of landforms and vegetation types representative of Mediterranean lowlands (see Table 1 for a comprehensive list of land cover types). Climate is Mediterranean subhumid and has a well-defined seasonality, with mild and wet winters and dry and hot summers. Mean annual precipitation is 550 mm, with rainfall displaying a sharp seasonality being mostly concentrated between October and March (80%) and almost absent between June and August.

Two different protection figures are included in the study area, the Doñana National and Natural Parks. The Doñana National Park is one of the most emblematic protected areas in Europe for its rich biotic diversity (e.g. Fernández-Delgado, 2006). It is strictly protected and only few, low-intensity traditional activities are allowed. The Doñana Natural (i.e. Regional) Park was initially created to buffer human impacts on the National Park. Here, a larger array of traditional practices is allowed including forestry, cattle ranching and game, and agriculture in some areas. Lastly, the region also includes non-protected areas that experienced a great agricultural transformation and intensified land use.

Two broad environmental units are represented in all protected and non-protected areas: the *Cotos* constituted by sandy soils of eolian origin and basal sands and slimes, and the *Marismas* (marshes) on clayish soils which originated after the filling of the Guadalquivir River old estuary. Vegetation in the *Cotos* has been transformed for centuries, resulting in a dramatic reduction of native cork-oak (*Quercus suber*), ash (*Fraxinus angustifolia*) poplar (*Populus alba*) and juniper (*Juniperus phoenicea*) woodlands and their replacement by scrubland formations dominated by Cistaceae (mostly *Halimium halimifolium*) and heathers (*Calluna vulgaris* and *Erica* spp.). Evergreen shrubs of *Pistacia lentiscus* and *Myrtus communis* are also found in some reduced areas. Since the XVII century some pines (*Pinus pinea*) are planted in the *Cotos*. More recently (1940s–1980s), larger extensions were afforested with pines and *Eucalyptus* spp. for wood and pine nut production. Simultaneously, most of the *Marismas* were drained and cultivated under both irrigation (rice fields) and non-irrigation (herbaceous crops), while water inputs in the natural marsh within protected areas have been altered from mostly alluvial to mostly pluvial.

2.2. Data collection

We used a representative sample of Landsat ETM+ satellite images covering one complete hydrological year (from October to September) between 2002 and 2003. The selected period represents a typical year in both the amount and seasonal distribution of rainfall: total precipitation in the study period was 549.5 mm of which 36% occurred in autumn, 44% in winter and 20% in spring, whereas the median for yearly precipitation over the period 1979–2003 was 548.6 mm, 34% in autumn, 45% in winter and 21% in spring. Therefore we expected to capture the most representative yearly patterns of ecosystem functioning in the region despite high interannual variability may also occur. Additionally, the reason to select one

Table 1
List of land use and land cover (LULC) types in the Doñana region, SW Spain.

1st level 3 classes	2nd level 8 classes	3rd level 18 classes	4th level 40 classes
Wetlands (w)	w·1 Marsh	w·11 Marsh	Tidal marsh; non-tidal marsh; bare marsh
		w·12 Salt marsh	Salt marsh
	w·2 Other wetlands	w·21 Riparian vegetation	Gallery forests; other riparian vegetation
		w·22 Seasonal lagoons	Seasonal lagoons
Agricultural areas (a)	a·1 Homogeneous agricultural areas	a·11 Homogeneous woody crops	Non-irrigated crops; irrigated crops
		a·12 Homogeneous herbaceous crops	Rice crops; other irrigated crops; non-irrigated crops
	a·2 Heterogeneous agricultural areas	a·21 Heterogeneous woody crops	Non-irrigated crops; irrigated crops
		a·22 Heterogeneous herbaceous crops	Herbaceous crop mosaics
		a·23 Crop mosaics with natural vegetation	Crop mosaics with natural vegetation
Natural and forested areas (n)	n·1 Forest	n·11 Dense forests	Broadleaved; conifers; eucalyptus; mixed
		n·12 Sparse forests with dense shrubland	Broadleaved; conifers; eucalyptus; mixed
		n·13 Sparse forests with sparse shrubland	Broadleaved; conifers; eucalyptus; mixed
		n·14 Sparse forests with pastures	Mixed broadleaved and pastures; mixed conifers and pastures; mixed eucalyptus and pastures; other mixtures
	n·2 Shrubland	n·21 Dense shrubland	Dense shrubland
		n·22 Disperse shrubland	Mixed shrubs and pastures; shrubs and bare soil
	n·3 Grassland	n·31 Grassland	Continuous grassland; grassland with bare soil
	n·4 Low vegetation cover	n·41 Sandy areas	Dunes and beaches
		n·42 Bare soils	Bare soil; Burned areas

The LULC classification was hierarchically organized into four levels of classification detail (Modified from Moreira, 2007). We used the 3rd hierarchical level with 18 classes for analyzing the correspondence between functional classes and LULC types.

representative year instead of a longer series of data was to avoid potentially spurious effects of temporal ecosystem functional changes (e.g. associated to land cover transformations) on the characterization of the spatial heterogeneity in ecosystem functioning.

Landsat images were chosen because they provide fine-grained data necessary for detecting high levels of spatial heterogeneity expected in Mediterranean environments – pixel size is 30 m for all bands except for the thermal band of 60 m – and the multi-spectral information required for calculating several integrative ecosystem indices. In contrast, the temporal resolution of our analysis is coarse due to the low frequency of satellite data acquisition. We selected five cloud-free images, each representing one study season, from summer 2002 to summer 2003. Images were dated on 18/07/02, 01/11/02, 10/01/03, 18/05/03 and 14/08/03, time of acquisition 10:50 h UTC. Radiometric data were corrected for atmospheric effects using dark-object subtraction in non-thermal bands (Chavez, 1989) and a mono-window algorithm in the thermal band (Qin et al., 2001). Images were geometrically referenced and corrected using a second-order warp function with 40 control points, achieving a mean-squared transformation error <1 pixel. The geometric correction was carried out after calculating all functional indices from each image (see below) in order to minimize wrapping effects on these calculations. All corrections were performed using the ENVI V.4.2 package.

2.3. Estimation of functional parameters

We used three integrative indexes of the energy balance of the land surface to define ecosystem functional types: the Normalized Difference Vegetation Index (NDVI) indicative of primary production, the land surface brightness temperature (T_s), related to heat partition, and the albedo, informing on reflection of the incoming radiation. In a first step, we did not include other ecosystem variables like fPAR or evapotranspiration in order to achieve classifications with minimal field data requirements and the least amount of assumptions and transformations. NDVI was estimated as follows:

$$NDVI = (NIR - RED) / (NIR + RED)$$

where *RED* and *NIR* stand for the spectral reflectivity acquired in the red and near-infrared wavelength intervals (Rouse et al., 1974), i.e. bands 3 (0.63–0.69 μm) and 4 (0.76–0.90 μm) of Landsat images respectively. This index measures the relative greenness of vegetation capturing the low vegetation reflectance in the red spectral region due to chlorophyll absorption and the dominant high reflectance in the near-infrared in plant tissues. NDVI is linearly related to the fraction of photosynthetically active radiation (Sellers et al., 1992) and hence to the leaf area index (Curran, 1983), vegetation biomass (Tucker et al., 1985) and net primary production (Prince, 1991). T_s was estimated converting reflectivity values in the thermal band 6 (10.40–12.50 μm) to at-sensor bright temperature (in Kelvin degrees; Landsat Project Science Office, 2008), and then applying the mono-window algorithm proposed by Qin et al. (2001). We matched the thermal data to the pixel size of other bands (30 m) sampling the image with no interpolation (i.e. every quartet of the resulting pixels has the same value of T_s). Lastly, albedo was estimated from bands 1 (blue, 0.45–0.52 μm), 3, 4, 5 (1.55–1.75 μm) and 7 (2.08–2.35 μm) following the formula derived by Liang (2001) for Landsat ETM+ after decoupling surface reflectance spectra from radiative transfer simulations:

$$Albedo = 0.356B1 + 0.130B3 + 0.373B4 + 0.085B5 + 0.072B7 - 0.0018$$

Changes in the magnitude of albedo have important climatic and biophysical consequences, being one of the most important attributes for characterizing the surface energy balance (Dickinson, 1995).

We estimated three first-order parameters from each reflectivity index and for every pixel of the image composite; these were the annual mean, maximum and range (i.e. maximum–minimum values) for the period between autumn 2002 and summer 2003 (i.e. one complete year). Then we estimated four second-order variables informing about ecosystem functional phenology, described as the daily rate of change between consecutive seasons for the period between summer 2002 and summer 2003 (i.e. all seasonal transitions in one year). This rate was calculated as the difference between one season and the next divided by the number of days between satellite scenes. In total each pixel was characterized by 21 functional variables corresponding to three first-order and four second-order derivations of NDVI, T_s and albedo data.

2.4. Definition of ecosystem functional types

We classified the observed variability in ecosystem functioning using clustering methods of data aggregation. For computational

limitations we used a sub-sample of one of every 4 pixels in both axes of the image. We standardized the data subtracting by the mean and dividing by the absolute deviation and estimated dissimilarity among observations calculating the Euclidian distance from the 21 variables. Data was finally clustered using the Clara algorithm (Kaufman & Rousseeuw, 1990), a non-hierarchical classification method based on partitioning around medoids (PAM). PAM searches for a number k of representative medoids in the data, i.e. data coordinates defining the central position of each cluster which minimizes the sum of dissimilarities among all cluster observations. Clara allows finding optimal medoids in large datasets by achieving PAM sub-samples of fixed size, and then assigns observations to the nearest optimal medoid to generate k clusters of data. Compared to other partitioning methods, Clara is more robust to extreme observations and noise, a frequent problem in remote sensing data.

One critical issue was deciding the optimal number of clusters k for aggregating the observed variability in the data. Most ecological classifications introduce some degree of subjectivity by either selecting k prior to data analysis (e.g. on the basis of verbal class descriptions) or specifying an arbitrary numerical threshold for the cluster distance estimates. In our study we intended to avoid any subjective delimitation of ecosystem functional types by using the Gap statistic (Tibshirani et al., 2001), a method that compares the change in within-cluster dispersion for a specified range of k with that expected under an appropriate null distribution. In essence, this method produces B uniform datasets for every k, computes the pooled within-cluster sum of squares around the cluster means (W_k) and compares it with its expectation under the null reference distribution (B). Gap(k) is the difference between the expected and observed $\log(W_k)$, and the standard deviation SD_k is estimated from the reference distribution. We selected the uniform reference distribution aligned with the principal components of the data, therefore avoiding assumptions about the shape of the data (Tibshirani et al., 2001). In our procedure, we simulated classifications varying k between 1 and 35 clusters and using $B=100$ Monte-Carlo reference distributions. The optimal number of clusters was the smallest k that satisfied the following two equations:

$$Gap(k) \geq Gap(k+1) - 1.96 S_{k+1}$$

$$Gap(k) \geq Gap(k+2) - 1.96 S_{k+2}$$

where:

$$S_k = SD_k \sqrt{1 + 1/B}$$

The optimal k was retained to identify ecosystem functional types from the clustered sub-sample of one of every 4 pixels. EFTs were finally mapped after classifying the complete image applying maximum-likelihood supervised classification (Richards, 1999) using the cluster observations as training data. Gap and cluster analyses were programmed in the R-statistical package V.2.1 (R Development Core Team, 2005).

2.5. Characterization of ecosystem functional types

Functional differences among EFTs were first explored by examining their position in the multidimensional space formed by the 21 functional variables using multiple discriminant analysis (e.g. Legendre & Legendre, 1998). We then examined the functional phenology for each type attending to two ecosystem parameters calculated from the original indices and meteorological data: the fraction of photosynthetic active radiation intercepted by vegetation (fPAR) and evapotranspiration (ETP). NDVI is approximately linearly related to fPAR (Ruimy et al., 1994), a direct indicator of aboveground primary production (Running et al., 2000). For each image date, we calculated the mean incoming radiation from data acquired in four weather stations located in the study area. Then, we explored the seasonal behaviour of fPAR in each functional type from the class means. Second, ETP was estimated from remote sensing data using the so-called simplified method as follows (Carlson et al., 1995):

$$ETP = Rn - B(T_s - T_a)^n$$

Where Rn is the net radiation, T_a is the air temperature and B and n are parameters that vary with vegetation. We estimated Rn from geometrical calculations of solar radiation and surface albedo following the procedure described in Nosetto et al. (2005). B and n were calculated from models based on NDVI data (Carlson et al., 1995), and T_a was averaged from data collected in four weather stations at the time of satellite data acquisition. Seasonality in fPAR and ETP was finally examined for each ecosystem functional type based on their average behaviour.

2.6. Correspondence between functional and structural classifications

We explored the association between EFTs and vegetation structure using correspondence analysis (CA; Legendre & Legendre, 1998). The vegetation composition of each functional type was estimated using a land use/land cover map of Southern Spain for the year 2003 (Moreira, 2007). This map was produced from the visual image interpretation of color and panchromatic ortophotos of 1 m and 0.5 m resolution, respectively, and supported with a temporal series of Landsat images covering the production year for differentiating highly seasonal land cover types (especially crop types). The map scale is 1:25,000 with minimum recognition units of 2500 m^2 and the documented classification accuracy is >94% (Moreira, 2007). The map information is organized in four different hierarchical levels of classification. For clarity, we re-arranged the hierarchical classification into four levels and analyzed the third classification level which represents a compromise between detail and generality in class descriptions (see Table 1). Correspondence analysis was performed on the cross-tabulation table of class-area frequencies calculated from the sub-sample of one of every 4 pixels. The relative agreement between ecosystem functional types and structural classes was then evaluated exploring the amount of inertia accounted for in each dimension of the CA, a measure of the sum of eigenvalues that reflects the spread of class points around the centroid. Finally, the relationship between functional and structural classifications was assessed by visual exploration of the two-dimensional plot of class coordinates together with the examination of the proportion of each land cover class within each EFT.

3. Results

3.1. Diversity of ecosystem functional types

The gap analysis indicated that the best separation of ecosystem functional types was achieved at $k=8$ clusters (see Appendix A, Fig. A1). However, the gap curve pointed to other local solutions of less separated groups at $k=19$ and $k=28$. The existence of several solutions is in agreement with the essence of ecosystem heterogeneity where patterns can be recognized at different levels of complexity and spatial detail. Here we focused on the primary classification with eight groups (Fig. 1).

We numbered EFTs attending to the cluster similarities among them (Fig. 2); for example, EFT.1 and EFT.2 were closely related whereas EFT.8 showed the highest dissimilarity with all other functional types. EFTs.1–4 were characterized by relatively high annual NDVI means (Fig. 3) although EFT.1 and EFT.2 were unique in showing clear NDVI increases in autumn. These were the most abundant functional types in the Doñana region whereas EFT.3 and

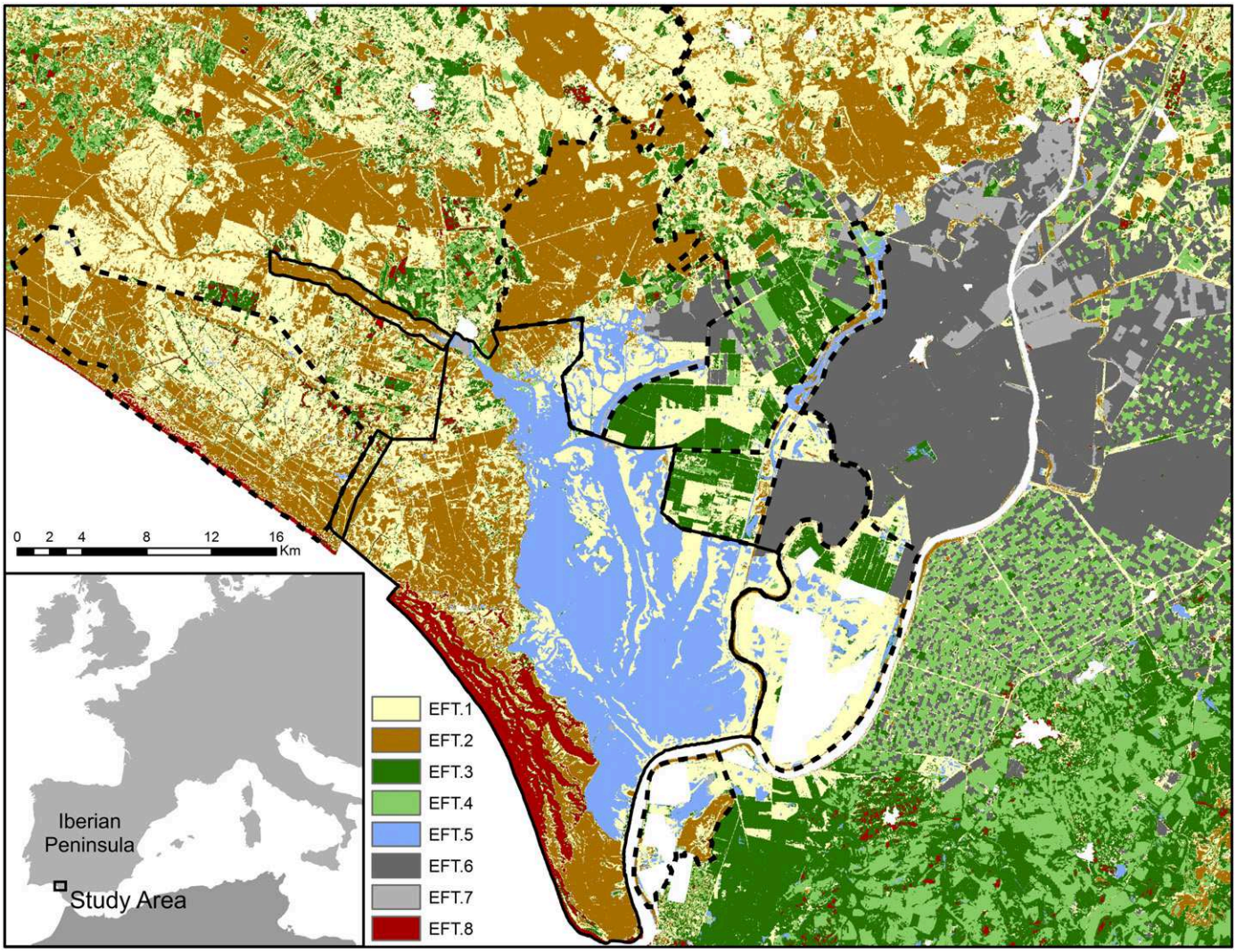

Fig. 1. Distribution of ecosystem functional types (EFTs) in the Doñana region, southwestern Spain. Colors represent the different EFTs (1–8; see legend) derived from the classification of Landsat ETM images attending to NDVI, albedo and surface temperatures in the hydrological year 2002–2003. The solid line shows the limits of the Doñana National Park and dashed lines show the different sectors of the Doñana Natural Park. White areas are masked areas of ocean (southwest), inland water bodies, and urban areas.

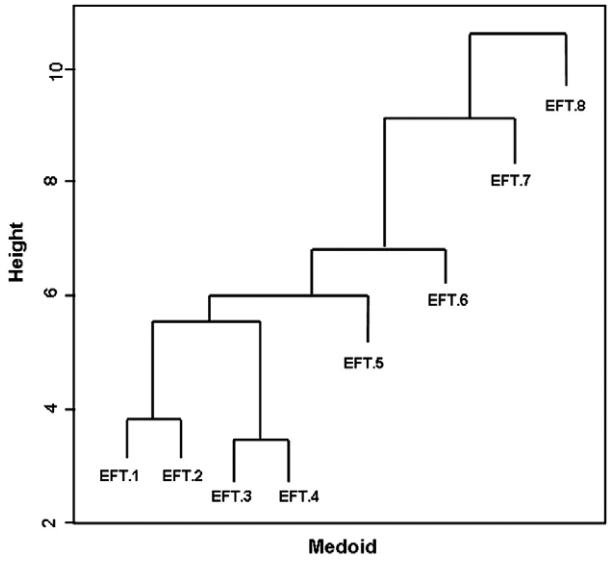

Fig. 2. Similarity among ecosystem functional types (EFTs) of the Doñana region resulting from the hierarchical cluster of medoids. Medoids represent the central position of each EFT minimizing the sum of dissimilarities among all observations.

EFT.4 were relatively abundant only in non-protected areas (Table 2). EFT.5 was characterized by clear increases in surface temperature and decreases in NDVI in summer contrasting with EFTs. 6–8 (results not shown). EFT.7 and EFT.8, the best separated in the cluster, were the rarest in terms of representativeness each occupying <3% of the total area (Fig. 2 and Table 2).

Annual average values of NDVI, T_s and albedo contributed more to the differentiation among ecosystem functional types than maximum and range statistics (Appendix A, Table A1 and Fig. A2). In the canonical discriminant analysis, the first canonical root separated mostly EFT.8, characterized by high albedo and low NDVI means, and EFT.2 and EFT.7 with relatively low T_s and albedo (Fig. 3). EFT.5, EFT.6 and EFT.7 were separated in the second root coinciding with low NDVI and T_s averages. The third root mostly discriminated EFT.4 and EFT.6, with a high yearly variation in NDVI and low variation in albedo, from EFT.5 with the opposite behaviour (Fig. 3).

The discriminant analysis on seasonal functional variables separated first the EFT.6 and EFT.7 associated with characteristic increases in NDVI in summer and parallel decreases in T_s (Appendix A, Fig. A2). The second root clearly discriminated EFT.2, EFT.5 and EFT.7, all showing large albedo increases in summer and comparatively low T_s increases in spring. The third root mostly contributed to discriminate EFTs with clear NDVI increases in autumn.

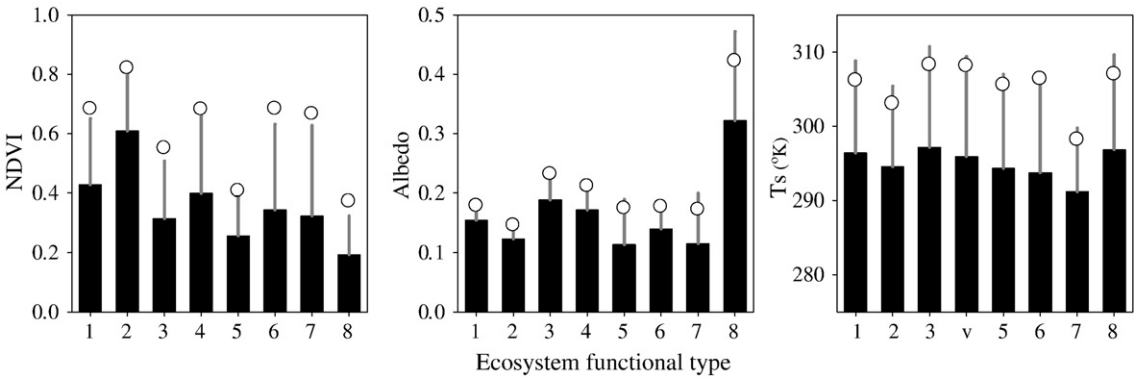

Fig. 3. Annual mean (histograms), maximum (empty dots) and range (bars) statistics for three ecosystem functioning variables characterizing ecosystem functional types (EFTs) in Doñana. Graphs represent EFT averages for the hydrological year 2002–2003.

3.2. Correspondence between ecosystem functional types and land cover

The combined ordination of EFTs and structural classes in three dimensions explained 87.9% of the total inertia in the correspondence frequency data. The first dimension reflected a gradient associated to vegetation density and seasonality, ranging from ephemeral herbaceous crops distributed in the right-side of the axis; perennial grasslands, sparse shrubs and woody crops in the centre; and dense shrubs and forests to the left (Fig. 4). The second dimension mostly separated sandy dunes in one end and seasonal wetlands (lagoons and marshes) in the other, whereas the third dimension (not shown) mostly separated between dunes and densely vegetated land cover types. We observed a clear association between some EFTs and specific land cover types (Fig. 4); for example, 82% of the area covered by sandy dunes coincided with EFT.8, whereas EFT.5 was present almost exclusively in wetlands (mostly marsh, Table 3). Four functional types – EFT.3, EFT.4, EFT.6 and EFT.7 – were specific of herbaceous crops, illustrating the high functional heterogeneity of these systems. On the contrary, EFT.1 was dominant in 10 different land cover types, from woody crops to various types of natural vegetation with low tree cover, which suggests a low functional specificity of these types. EFT.2 was dominant in natural perennial vegetation, mostly dense forests (nearly 70% of forests corresponded to this type), sparse forests with dense shrubs and dense riparian vegetation (Fig. 4 and Table 3).

3.3. Seasonality in fPAR and ETP

Typically, the Doñana ecosystems showed a gradual decrease in evapotranspiration from summer (>3 mm day^{-1}) to winter (<0.5 mm day^{-1}) and subsequent increases in spring. However, we noticed relevant differences among ecosystem functional types (Fig. 5). The lowest evapotranspiration occurred in EFT.8 with values close to 0 in winter and autumn and increasing to only 2.4 mm day^{-1} in summer. EFT.6 and EFT.7 showed the highest evapotranspiration in summer (4.6 mm day^{-1}) and also the largest annual variability (4.3 mm day^{-1}). The transition from winter minima to summer peaks was also highly variable, with major increases in spring in EFT.4, EFT.5 and EFT.7 and in winter in EFT.6 and EFT.8.

Although annual evapotranspiration and T_s were correlated (Spearman's $r=0.72$; $P<0.001$), their dynamics were not always equivalent. For example, mean and maximum surface temperatures were lower in EFT.2 than in EFT.1 (Fig. 3) but evapotranspiration was always higher in the former (Fig. 5). The opposite was observed for EFT.5 with relatively high temperatures and low evapotranspiration, and EFT.7 with low temperatures but high evapotranspiration particularly in summer.

Seasonal differences among ecosystem functional types were even more notorious for fPAR. For example, fPAR peaked in winter in EFT.1, EFT.2, EFT.3 and EFT.8 but only EFT.1 and EFT.2 displayed a well-defined bell-shaped curve with a clear autumn increase and a subsequent gradual decrease from winter to summer. In contrast, EFT.4 and EFT.5 peaked in spring, whereas EFT.6 and EFT.7 showed two peaks, one in summer coinciding the date of maximum ETP and a second, lower peak in winter (Fig. 5).

Table 2
Representativeness (in km^2) of ecosystem functional classes in differently protected areas of the Doñana region, SW Spain.

Functional type	National Park	Natural Park	Unprotected	Total
EFT.1	133.7 (25.9%)	203.0 (40.7%)	690.0 (27.1%)	1026.6 (28.8%)
EFT.2	119.6 (23.2%)	177.7 (35.6%)	400.6 (15.7%)	697.9 (19.6%)
EFT.3	13.2 (2.6%)	47.1 (9.4%)	477.1 (18.7%)	537.4 (15.1%)
EFT.4	4.3 (0.8%)	7.3 (1.5%)	350.7 (13.8%)	362.3 (10.2%)
EFT.5	197.7 (38.4%)	35.7 (7.2%)	11.6 (0.5%)	245.1 (6.9%)
EFT.6	0.6 (0.1%)	15.0 (3.0%)	519.1 (20.4%)	534.7 (15.0%)
EFT.7	1.8 (0.3%)	3.8 (0.8%)	62.7 (2.5%)	68.3 (1.9%)
EFT.8	44.6 (8.7%)	9.4 (1.9%)	35.3 (1.4%)	89.3 (2.5%)

Percentages in brackets refer to percent area within each protection status.

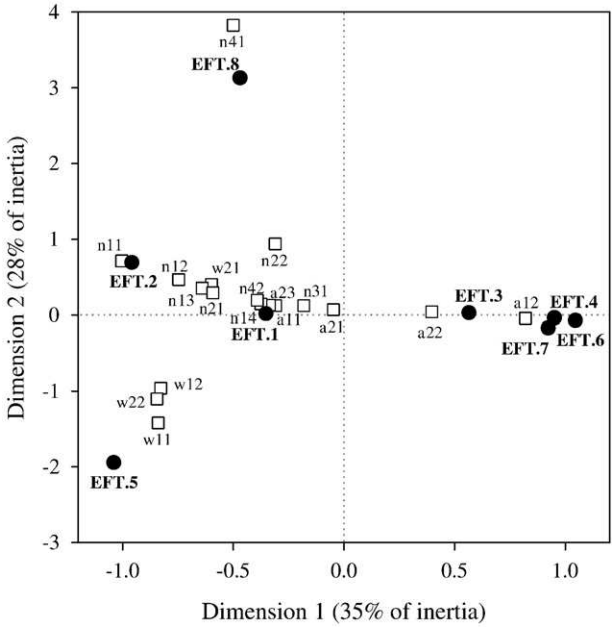

Fig. 4. Diagram of correspondences between ecosystem functional types (EFTs) and land cover classes in the Doñana region. The diagram results from the correspondence analysis on the cross-tabulation table of area frequencies. Land cover classes are detailed in Table 1; w stands for wetlands; n = forests and other natural areas; a = agricultural areas.

Table 3
Proportion of the area occupied by eight ecosystem functional types (EFTs) in the different land cover classes of the Doñana region.

Code	Land cover	EFT.1	EFT.2	EFT.3	EFT.4	EFT.5	EFT.6	EFT.7	EFT.8
w·11	Marsh	40.7	2.5	4.6	0.8	49.3	1.5	0.5	0.1
w·12	Salt marsh	57.6	6.4	0.0	0.0	35.0	0.0	1.1	0.0
w·21	Riparian vegetation	33.8	46.5	4.5	3.3	2.8	7.8	1.0	0.3
w·22	Seasonal lagoons	26.6	18.6	1.7	1.0	43.6	0.1	8.2	0.2
n·11	Dense forest	29.7	68.2	1.5	0.2	0.0	0.0	0.0	0.2
n·12	Sparse forest, dense shrubland	53.2	41.4	3.9	0.8	0.0	0.0	0.0	0.8
n·13	Sparse forest, sparse shrubland	62.5	30.5	5.8	0.4	0.0	0.1	0.0	0.8
n·14	Sparse forest with pasture	70.4	13.3	14.9	1.0	0.2	0.2	0.0	0.1
n·21	Dense shrubland	65.3	25.9	5.2	1.9	0.8	0.0	0.0	0.9
n·22	Disperse shrubland	52.5	8.6	18.1	2.1	0.4	0.1	0.0	18.2
n·31	Grassland	54.1	12.6	24.6	5.0	1.9	0.8	0.2	0.9
n·41	Sandy areas	3.8	1.7	10.0	0.2	1.9	0.2	0.0	82.2
n·42	Bare soil	42.6	26.0	23.2	1.0	4.4	0.0	1.6	1.1
a·11	Homogeneous woody crops	71.1	9.7	17.8	1.0	0.0	0.2	0.0	0.3
a·12	Homogeneous herbaceous crops	17.4	1.6	26.4	18.7	0.5	31.2	3.9	0.2
a·21	Heterogeneous woody crops	59.0	4.7	32.7	3.1	0.0	0.2	0.0	0.3
a·22	Heterogeneous herbaceous crops	34.9	3.2	35.6	20.7	0.2	4.8	0.0	0.5
a·23	Crops with natural vegetation	66.4	13.8	13.5	4.7	1.0	0.3	0.0	0.3

w stands for wetlands; n = forests and other natural areas; a = agricultural areas.

4. Discussion

The approach presented here is novel in identifying ecosystem heterogeneity from a combination of functional parameters that capture the main components of the carbon, energy and water balances in the land surface. We expanded the concept of "ecosystem functional type" originally proposed on the basis of carbon gains (Paruelo et al., 2001b) and included indicators of energy partitioning into sensible and latent heat fluxes and light reflection (Krustas & Norman, 1996; Liang, 2001), making it more comprehensive for identifying multifunctional patterns associated to both biomass production and feedbacks on climate. Moreover, we achieved a numerical classification of the variability in ecosystem functioning therefore reducing subjectivity in the process of class identification (Host et al., 1996). This provided a unique perspective on the ecosystem heterogeneity independent of structural ecosystem classifications and other subjective characterizations.

4.1. Spatial heterogeneity in ecosystem functioning

Mediterranean ecosystems of the Doñana region displayed pronounced gradients in all the functional descriptors studied. These gradients were strong even within the less human-modified areas: for example, considering exclusively ecosystem functional types of the National Park, the mean annual maximum NDVI varied from 0.35 (EFT.8) to 0.86 (EFT.2). This difference is similar to the values reported at the biome level, e.g. between humid forests and semi-arid steppes in South America (Paruelo et al., 2004b). Other functional parameters showed consistent patterns, with differences of > 2 °C in annual mean, maximum and range temperatures in the land surface, and up to three-times differences in albedo (EFT.8 mean = 33.6% vs. EFT.2 mean = 11.7%). Previous studies conducted at broader spatial scales have emphasized the role of bioclimatic controls as key determinants of ecosystem functional diversity (Lobo et al., 1997; Suzuki et al., 2000; Paruelo et al., 2001b; Alcaraz et al., 2006). By controlling for the effect

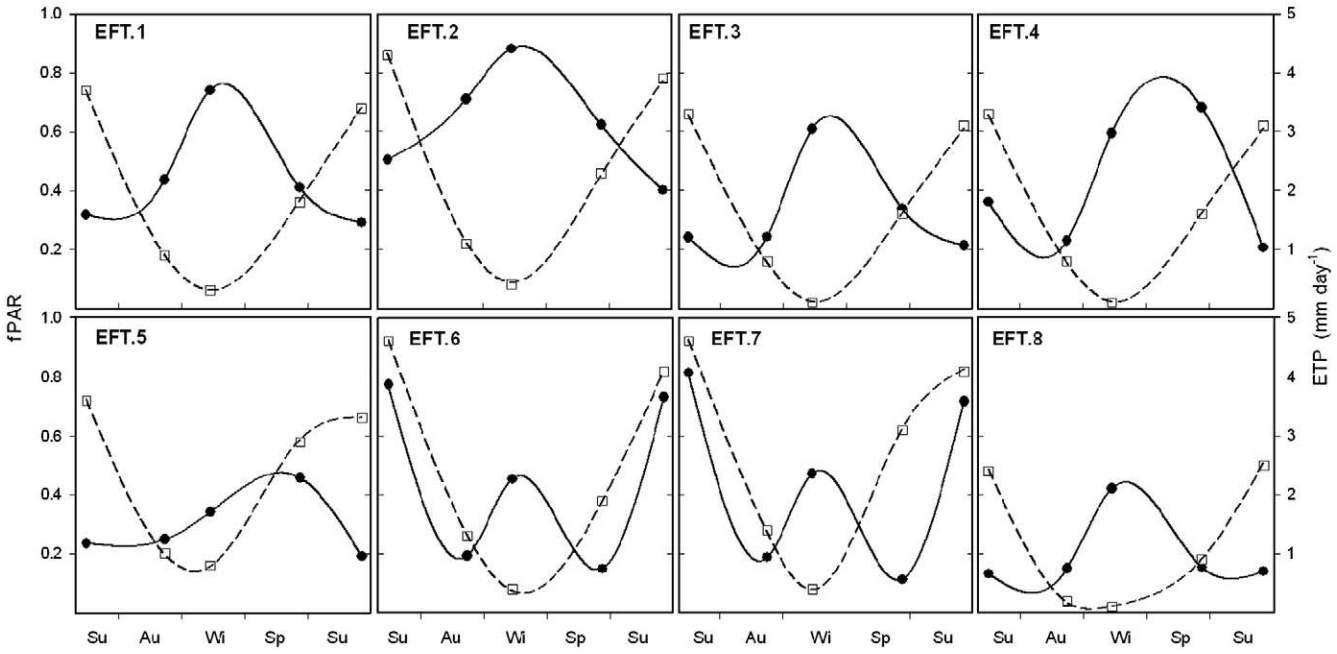

Fig. 5. Functional phenology of the Doñana ecosystem functional types (EFTs) during the hydrological year 2002–2003. fAPAR (solid line) is the fraction of Absorbed Photosynthetically Active Radiation and ETP (dashed line) is the rate of evapotranspiration in the land surface.

of bioclimatic variability we showed that local controls produce highly heterogeneous functioning patterns in Mediterranean environments: high local variability occurred within a relatively small region with negligible variations in climate.

The spatial distribution of ecosystem functional types was partly associated to the protection status. This agreed with the well-established hypothesis that ecosystem functioning is critically modified by human land use. For example, three functional types almost exclusive of non-protected areas showed dramatic seasonal shifts in fPAR dynamics (EFT.4, EFT.6 and EFT.7) together with larger increases in evapotranspiration in summer (EFT.6 and EFT.7). Changes in these features may have important effects on the local climate that will require further analyses. However, differences were not so obvious when exploring yearly synthetic ecosystem parameters, indicating a low impact of human transformations on these descriptors as compared to natural variability (see also Guerschman et al., 2003). Moreover, human use intensity did not always imply profound modifications of seasonal ecosystem functioning. For example, EFT.1 and EFT.2 were well represented in both protected and non-protected areas covering a large array of natural and human-exploited vegetation types with similar ecosystem functioning. Seasonality patterns in these classes were consistent with the water-limitation hypothesis in Mediterranean ecosystems (Piñol et al., 1995): fPAR closely followed the yearly distribution of precipitation and evapotranspiration experimented dramatic summer increases (EFT averages $\geq$3.4 mm day^{-1}). The strong limitation imposed by water availability would mask the anthropic effect on ecosystem functioning.

Lastly, only two functional types were almost exclusively present in protected areas: EFT.5 (associated to dunes and other sandy areas) and EFT.8 (in natural marshes) displayed comparatively low yearly fPAR values. fPAR averages in EFT.5 were similar to Mediterranean semi-arid environments with much lower rainfall ($<$200 mm; Paruelo et al., 2005). On the other hand, the particular seasonal course of fPAR in EFT.5 was clearly associated to alternate flooding and extreme drought periods in clayish natural marshes: soil permeability probably determined very specific patterns in seasonal ecosystem water limitation both in natural marshes and sandy dunes.

4.2. Correspondence between functional heterogeneity and land use and cover

Our study revealed that heterogeneity patterns in ecosystem functional and structural properties are not necessarily analogous. First, we found a high variety of natural vegetation types associated to a reduced number of functional profiles. This occurred in the *Cotos* present in the two natural protected areas. Here, different vegetation formations including grassland, various types of shrubland, riparian forests and pine forests displayed a low functional variability covered by only two ecosystem functional types. Moreover, the same types comprised heavily modified areas like afforestations and orchads. In contrast, a relatively small portion of the landscape (sandy dunes and deep marshes) contained two specific EFTs, highlighting their uniqueness not only from structural but also from the functional perspective. On the other hand, structurally much simpler vegetation formations in agricultural areas accounted for most functional variability outside protected areas. Their functional characteristics suggest that human activities exceed natural ecosystem controls creating unique new patterns in the water, energy and carbon balance of Mediterranean environments.

Different studies showed the key influence of land use on various ecosystem functioning parameters at regional scales (e.g. Houghton et al., 1999; Bounoua et al., 2002; Nosetto et al., 2005). However, few of them addressed the variable consequences of human alterations on water and energy budgets in relation to the ecological setting and the type of land use, an issue with important implications for understanding the ecological costs of human activities (DeFries et al., 2004). Although we did not address temporal changes in ecosystem functioning, the analysis of ecosystem functional types in relation to land use revealed contrasting consequences of human activities depending on the ecological settings. For example, cropping in estuarine areas generated the most dramatic alteration of the annual pattern of NDVI and fPAR, increasing annual averages and modifying profoundly seasonal dynamics as compared to natural marshland. Annual fPAR did not differ between herbaceous crops and shrubland but herbaceous crops presented higher surface temperature and albedo, two attributes that may contribute to alter local climate (Wang & Davidson, 2007). In general, the functional patterns observed in woody crops and afforestations did not differ from other natural areas attending to our classification, which suggests that these activities had a lower impact on water and energy exchange than other land cover transformations. However, the primary level of class segregation analyzed here may have overlooked more subtle functional differences between some heavily humanized and less transformed ecosystems.

5. Conclusions

The co-occurrence of water limitation and high temperatures in summer typical of Mediterranean environments probably represents one of the most critical factors influencing ecosystem functioning in most natural areas of Doñana, controlling seasonal patterns of primary production and causing high evapotranspiration rates and water deficits. Variations around this pattern seem to be ultimately associated to landform and its effects on groundwater availability and vegetation structure, generating differing functioning patterns in marshes dominated by alternate flooding and drought periods; in dunes characterized by low vegetation cover and water holding capacity; and in the *Cotos* where a high diversity of evergreen vegetation formations are present. This finding generated a partial correspondence between ecosystem structural characteristics and functioning. However, a large variety of natural vegetation types present in the *Cotos* were classified within two ecosystem functional types. Moreover, human activities in different ecological settings have increased the functional diversity of Mediterranean environments, producing severe alterations in the seasonal dynamics of primary production and on the water and energy balances in the land surface.

It has been proposed that natural protected areas provide a unique reference situation where ecosystem functioning reflects the baseline conditions necessary to evaluate the impact of human activities outside these areas (Garbulsky & Paruelo, 2004; Alcaraz-Segura et al., 2009). Some great functional differences between protected areas and nearby transformed land in Doñana suggest that land use is a key driver of biogeochemical processes at the local level. Our analyses in Doñana show that both the ecological context and the type of land use strongly influence the direction and magnitude of functional changes associated to human activities. This finding emphasizes the need to expand ecosystem functional analyses to understand the effects of natural variability and land use on primary processes of matter, energy and water dynamics. However, the use of protected areas for evaluating ecosystem changes should carefully consider potential biases associated to the overrepresentation of “rare” ecosystem functional types not necessarily representative of typical reference conditions. The combined use of land cover and ecosystem functioning classifications can greatly help to define reference conditions and to track more comprehensively the ecosystem-level consequences of environmental change in many different environments.

Acknowledgments

Funding was provided by the Dirección General de Investigación, Tecnología y Empresa of Junta de Andalucía (Proyecto de Excelencia

#01288) and the Doñana, 2005 Program (Ministerio de Medio Ambiente y Junta de Andalucía). Satellite images were provided by the LAST at the Doñana Biological Station. We thank Mayra Milkovic, Mercedes Vasallo and Luciana Porfirio for helping with the data processing and two anonymous referees for their helpful comments on an earlier manuscript.

Appendix A. Supplementary data

Supplementary data associated with this article can be found, in the online version, at doi:10.1016/j.rse.2009.09.001.

References

Alcaraz-Segura, D., Cabello, J., Paruelo, J., & Delibes, M. (2009). Use of descriptors of ecosystem functioning for monitoring a national park network: A remote sensing approach. *Environmental Management*, *43*, 38−48.

Alcaraz, D., Paruelo, J., & Cabello, J. (2006). Identification of current ecosystem functional types in the Iberian Peninsula. *Global Ecology and Biogeography*, *15*, 200−212.

Bounoua, L., DeFries, R., Collatz, G. J., Sellers, P., & Khan, H. (2002). Effects of land cover conversion on surface climate. *Climatic Change*, *52*, 29−64.

Bradford, J. B., Lauenroth, W. K., & Burke, I. C. (2005). The impact of cropping on primary production in the US great plains. *Ecology*, *86*, 1863−1872.

Bradford, J. B., Lauenroth, W. K., Burke, I. C., & Paruelo, J. M. (2006). The influence of climate, soils, weather, and land use on primary production and biomass seasonality in the US Great Plains. *Ecosystems*, *9*, 934−950.

Camacho-De Coca, F., Garcia-Haro, F. J., Gilabert, M. A., & Melia, J. (2004). Vegetation cover seasonal changes assessment from TM imagery in a semi-arid landscape. *International Journal of Remote Sensing*, *25*, 3451−3476.

Carlson, T. N., Capehart, W. J., & Gillies, R. R. (1995). A new look at the simplified method for remote-sensing of daily evapotranspiration. *Remote Sensing of Environment*, *54*, 161−167.

Chapin, F. S., Randerson, J. T., McGuire, A. D., Foley, J. A., & Field, C. B. (2008). Changing feedbacks in the climate–biosphere system. *Frontiers in Ecology and the Environment*, *6*, 313−320.

Chavez, P. S. (1989). Radiometric calibration of Landsat thematic mapper multispectral images. *Photogrammetric Engineering and Remote Sensing*, *55*, 1285−1294.

Christensen, N. L., Bartuska, A. M., Brown, J. H., Carpenter, S., DAntonio, C., Francis, R., et al. (1996). The report of the ecological society of America committee on the scientific basis for ecosystem management. *Ecological Applications*, *6*, 665−691.

Cohen, W. B., & Goward, S. N. (2004). Landsat's role in ecological applications of remote sensing. *BioScience*, *54*, 535−545.

Crabtree, R., Potter, C., Mullen, R., Sheldon, J., Huang, S., Harmsen, J., et al. (2009). A modeling and spatio-temporal analysis framework for monitoring environmental change using NPP as an ecosystem indicator. *Remote Sensing of Environment*, *113*, 1486−1496.

Curran, P. J. (1983). Multispectral remote-sensing for the estimation of green leaf-area index. *Philosophical Transactions of the Royal Society of London Series A-Mathematical Physical and Engineering Sciences*, *309*, 257−270.

DeFries, R. S., Field, C. B., Fung, I., Collatz, G. J., & Bounoua, L. (1999). Combining satellite data and biogeochemical models to estimate global effects of human-induced land cover change on carbon emissions and primary productivity. *Global Biogeochemical Cycles*, *13*, 803−815.

DeFries, R. S., Foley, J. A., & Asner, G. P. (2004). Land-use choices: Balancing human needs and ecosystem function. *Frontiers in Ecology and the Environment*, *2*, 249−257.

Dickinson, R. E. (1995). Land processes in climate models. *Remote Sensing of Environment*, *51*, 27−38.

Fernández-Delgado, C. (2006). Conservation management of an European Natural Area: Doñana National Park, Spain. In M. J. Groom, G. K. Meffe & C.R. Carroll (Eds.), *Principles of Conservation Biology* (pp. 536−543)., Third Edition Sunderland, Massachusetts, USA: Sinauer Associates, Inc. Publishers.

Garbulsky, M. F., & Paruelo, J. M. (2004). Remote sensing of protected areas to derive baseline vegetation functioning characteristics. *Journal of Vegetation Science*, *15*, 711−720.

Gould, W. (2000). Remote sensing of vegetation, plant species richness, and regional biodiversity hotspots. *Ecological Applications*, *10*, 1861−1870.

Guerschman, J. P., Paruelo, J. M., & Burke, I. C. (2003). Land use impacts on the normalized difference vegetation index in temperate Argentina. *Ecological Applications*, *13*, 616−628.

Hill, J., Stellmes, M., Udelhoven, T., Roder, A., & Sommer, S. (2008). Mediterranean desertification and land degradation: Mapping related land use change syndromes based on satellite observations. *Global and Planetary Change*, *64*, 146−157.

Hooper, D. U., Chapin, F. S., Ewel, J. J., Hector, A., Inchausti, P., Lavorel, S., et al. (2005). Effects of biodiversity on ecosystem functioning: A consensus of current knowledge. *Ecological Monographs*, *75*, 3−35.

Host, G. E., Polzer, P. L., Mladenoff, D. J., White, M. A., & Crow, T. R. (1996). A quantitative approach to developing regional ecosystem classifications. *Ecological Applications*, *6*, 608−618.

Hostert, P., Roder, A., & Hill, J. (2003). Coupling spectral unmixing and trend analysis for monitoring of long-term vegetation dynamics in Mediterranean rangelands. *Remote Sensing of Environment*, *87*, 183−197.

Houghton, R. A., Hackler, J. L., & Lawrence, K. T. (1999). The US carbon budget: Contributions from land-use change. *Science*, *285*, 574−578.

Kaufman, L., & Rousseeuw, P. J. (1990). *Finding groups in data. An introduction to cluster analysis.* New York: Wiley.

Kerr, J. T., & Ostrovsky, M. (2003). From space to species: Ecological applications for remote sensing. *Trends in Ecology and Evolution*, *78*, 1−7.

Krustas, W. P., & Norman, J. M. (1996). Use of remote sensing for evapotranspiration monitoring over land surfaces. *Hydrological Sciences*, *41*, 495−516.

Landsat Project Science Office. (2008). Landsat 7 Science Data Users Handbook. http://landsathandbook.gsfc.nasa.gov/handbook/handbook_toc.html

Legendre, P., & Legendre, L. (1998). *Numerical Ecology*, Second edition Amsterdam, Nederland: Elsevier.

Liang, S. L. (2001). Narrowband to broadband conversions of land surface albedo: I. Algorithms. *Remote Sensing of Environment*, *76*, 213−238.

Lobo, A., Marti, J. J. I., & GimenezCassina, C. C. (1997). Regional scale hierarchical classification of temporal series of AVHRR vegetation index. *International Journal of Remote Sensing*, *18*, 3167−3193.

Melillo, J. M., Mcguire, A. D., Kicklighter, D. W., Moore, B., Vorosmarty, C. J., & Schloss, A. L. (1993). Global climate-change and terrestrial net primary production. *Nature*, *363*, 234−240.

Millennium Ecosystem Assessment. (2005). *Drivers of Change in Ecosystem Condition and Services. Chapter 7. Ecosystems and Human Well-Being: Scenarios* (pp. 173−222). Washington, D.C., USA: Island Press.

Moreira, J. M. (2007). Mapa de usos y coberturas vegetales de Andalucía Escala 1/25.000. Guia técnica. In (p. 207). Seville: Consejería de Medio Ambiente. Junta de Andalucía.

Nosetto, M. D., Jobbagy, E. G., & Paruelo, J. M. (2005). Land-use change and water losses: The case of grassland afforestation across a soil textural gradient in central Argentina. *Global Change Biology*, *11*, 1101−1117.

Noss, R. F. (1990). Indicators for monitoring biodiversity: a hierarchical approach. *Conservation Biology*, *4*, 355−364.

Paruelo, J. M., Burke, I. C., & Lauenroth, W. K. (2001). Land-use impact on ecosystem functioning in eastern Colorado, USA. *Global Change Biology*, *7*, 631−639.

Paruelo, J. M., Garbulsky, M. F., Guerschman, J. P., & Jobbagy, E. G. (2004). Two decades of Normalized Difference Vegetation Index changes in South America: Identifying the imprint of global change. *International Journal of Remote Sensing*, *25*, 2793−2806.

Paruelo, J. M., Golluscio, R. A., Guerschman, J. P., Cesa, A., Jouve, V. V., & Garbulsky, M. F. (2004). Regional scale relationships between ecosystem structure and functioning: The case of the Patagonian steppes. *Global Ecology and Biogeography*, *13*, 385−395.

Paruelo, J. M., Jobbagy, E. G., & Sala, O. E. (2001). Current distribution of ecosystem functional types in temperate South America. *Ecosystems*, *4*, 683−698.

Paruelo, J. M., Pineiro, G., Oyonarte, C., Alcaraz, D., Cabello, J., & Escribano, P. (2005). Temporal and spatial patterns of ecosystem functioning in protected and areas in southeastern Spain. *Applied Vegetation Science*, *8*, 93−102.

Pettorelli, N., Vik, J. O., Mysterud, A., Gaillard, J. M., Tucker, C. J., & Stenseth, N. C. (2005). Using the satellite-derived NDVI to assess ecological responses to environmental change. *Trends in Ecology & Evolution*, *20*, 503−510.

Piñol, J., Terradas, J., Avilas, A., & Ferra, A. (1995). Using catchments of contrasting hydrological conditions to explore climate effects on water and nutrient flows in Mediterranean forests. In J. M. Moreno & W.C. Oechel (Eds.), *Global change and Mediterranean-type ecosystems* New York: Springer.

Prince, S. D. (1991). A model of regional primary production for use with coarse resolution satellite data. *International Journal of Remote Sensing*, *12*, 1313−1330.

Qin, Z., Karnieli, A., & Berliner, P. (2001). A mono-window algorithm for retrieving land surface temperature from Landsat TM data and its application to the Israel–Egypt border region. *International Journal of Remote Sensing*, *22*, 3719−3746.

R Development Core Team (2005). *R: A language and environment for statistical computing* Vienna, Austria: R foundation for Statistical Computing.

Richards, J. A. (1999). *Remote Sensing Digital Image Analysis.* Berlin: Springer-Verlag.

Rouse, J. W., Haas, R. W., Schell, J. A., Deering, D. W., & Harlan, J. C. (1974). *Monitoring the vernal advancement and retrogradation (green-wave effect) of natural vegetation. Final Rep. RSC 1978-4* (pp. 93). : Remote Sensing Center, Texas A&M Univ., College Station.

Ruimy, A., Saugier, B., & Dedieu, G. (1994). Methodology for the estimation of terrestrial net primary production from remotely sensed data. *Journal of Geophysical Research*, *99*, 5263−5283.

Running, S. W., Thornton, P. E., Nemani, R. R., & Glassy, J. M. (2000). Global terrestrial gross and net primary productivity from the earth observing system. In R. J. O. Sala & H.A. Mooney (Eds.), *Methods in Ecosystem Science* New York: Springer-Verlag.

Sellers, P. J., Berry, J. A., Collatz, G. J., Field, C. B., & Hall, F. G. (1992). Canopy reflectance, photosynthesis, and transpiration. III. A reanalysis using improved leaf models and a new canopy integration scheme. *Remote Sensing of the Environment*, *42*, 187−216.

Soriano, A., & Paruelo, J. M. (1992). Biozones—Vegetation units defined by functional characters identifiable with the aid of satellite sensor images. *Global Ecology and Biogeography Letters*, *2*, 82−89.

Shoshany, M. (2000). Satellite remote sensing of natural Mediterranean vegetation: a review within an ecological context. *Progress in Physical Geography*, *24*, 153−178.

Suzuki, R., Tanaka, S., & Yasunari, T. (2000). Relationships between meridional profiles of satellite-derived vegetation index (NDVI) and climate over Siberia. *International Journal of Climatology*, *20*, 955−967.

Tibshirani, R., Walther, G., & Hastie, T. (2001). Estimating the number of clusters in a data set via the gap statistic. *Journal of the Royal Statistical Society Series B-Statistical Methodology*, *63*, 411−423.

Tucker, C. J., Townshend, J. R. G., & Goff, T. E. (1985). African land-cover classification using satellite data. *Science*, *227*, 369−375.

Turner, W., Spector, S., Gardiner, N., Fladeland, M., Sterling, E., & Steininger, M. (2003). Remote sensing for biodiversity science and conservation. *Trends in Ecology & Evolution*, *18*, 306−314.

Vitousek, P. M. (1994). Beyond global warming—Ecology and global change. *Ecology*, *75*, 1861−1876.

Wang, S. S., & Davidson, A. (2007). Impact of climate variations on surface albedo of a temperate grassland. *Agricultural and Forest Meteorology*, *142*, 133−142.